Journal of Sustainable Mining 16 (2017) 55–65

HOSTED BY

ELSEVIER

Contents lists available at ScienceDirect

Journal of Sustainable Mining

journal homepage: http://www.elsevier.com/locate/jsm

Research paper

Assessment of gas permeability coefficient of porous materials

Grzegorz Wałowski

Department of Renewable Energy Resources, Institute of Technology and Life Sciences, 67 Biskupińska Street, 60-463 Poznań, Poland

A R T I C L E I N F O

Article history:
Received 15 May 2017
Received in revised form
18 July 2017
Accepted 23 August 2017
Available online 30 August 2017

Keywords:
Gas permeability
Frame-structured porous material
Biogas
Raw gas

A B S T R A C T

The results of experimental research upon the assessment of gas permeability of porous materials with respect to the gas flow. The conducted research applied to natural materials with an anisotropic gap-porous structure and - for comparative purposes - to model materials such as pumice and polyamide agglomerates. The research was conducted with the use of a special test stand that enables measuring the gas permeability with respect to three flow orientations compared with symmetric cubic-shaped samples. The research results show an explicit impact of the flow direction on the permeability of biochar, which results from their anisotropic internal structures. The permeability coefficient of such materials was determined and an experimental evaluation of the value of this coefficient was conducted with respect to the gas stream and the total pressure drop across the porous deposit.

The process of gas permeability was considered in the category of hydrodynamics of gas flow through porous deposits. It is important to broaden the knowledge of gas hydrodynamics assessment in porous media so far unrecognised for the development of a new generation of clean energy sources, especially in the context of biogas or raw gas production.

1. Introduction

A large variety of porous deposits, both in terms of their use in the industrial technology, among others, leaching petroleum substances (Błaszczyk, 2014), cleaning the air from the volatile organic compounds (Iliuta & Larachi, 2005; Janecki, Gąszczak, & Bartelmus, 2016), bio-leaching black shale ores (Erust, Akcil, Gahan, Tusenuk, & Deveci, 2013; Barańska & Sadowski, 2015) and the occurrence in the natural environment – filtration (Darcy, 1856; Strzelecki, Kostecki, & Żak, 2008), movement of natural gases (e.g. methane) by rock masses (Krause, 2009), the flow of reaction gases from the thermal gasification in the georeactor (Gregg & Edgar, 1978; Smoliński, Stańczyk, Kapusta, & Howaniec, 2013) or retention in the process of underground bioconversion when selecting strains of microorganisms to achieve the maximum biogas efficiency (Stachowiak, Nowak, & Sztromwasser, 2011) makes the flow of fluids through this type of materials very complex and still not fully recognised. At the same time, the reference books are quite varied in its subject matter, where a greater emphasis is placed on the application of hydrodynamic of the fluid flow through porous deposits (whether granular or frame-structured) than on basic research.

Although the reference books widely analyse the gas flow through porous materials, they do not clearly interpret and explicitly indicate the nature of hydrodynamic phenomena accompanying this process. This mainly results from a very complex and diversified structure of porous materials which – due to changeable flow conditions – entails difficulties in interpreting those phenomena and – frequently due to the changeable process scale - from porous grains to porous deposits. And although the reference books do not lack models that consider structural features of porous materials in their descriptions, especially in the aspect of homogenisation theory (Auriault & Caillerie, 1989; Auriault & Royer, 1993; Auriault, Strzelecki, Bauer, & He, 1990; Łydżba, 1991, 2002), the impact of the anisotropic structure on the permeability of porous materials has not been sufficiently recognised. This situation becomes more complex with respect to the assessment of hydrodynamics of the gas flow through solid materials with porous (frame-structured) construction. At the same time, in this field it is difficult to find information on hydrodynamics of the gas flow through this type of porous materials.

In each case, the recognition of conditions of gas flow through porous deposits results in serious problems concerning the description of hydrodynamics and the evaluation of mechanisms of gas flow through those deposits, particularly due to their diversified construction and internal structure. On the other hand, by

E-mail address: walowski.g@gmail.com.

http://dx.doi.org/10.1016/j.jsm.2017.08.001

List of major signs

A	total cross-section of the flow channel (m^2)
F	cross-sectional area (m^2)
K	permeability coefficient (m^2)
L	flow path length describing the porous bad height (m)
Q	stream, volume flow rate (m^3/s)
d	diameter (m)
g	gravitational acceleration (m/s^2)
p	pressure (Pa)
u	apparent velocity (m/s)
β	parameter in this case indicates the deviation from the linear Darcy relationship, as caused by the additional kinetics effects ($1/m^2$)
ΔP	pressure drop (Pa)
ε	porosity
η	fluid viscosity (Pa·s)
ρ	density (kg/m^3)
ξ	coefficient of drag flow

Lower indices refer to

ASTM	acc. American Society for Testing and Materials
B	acc. Brinkman
D	acc. Darcy
Du	acc. Dullien
F	acc. Forchheimer
S	acc. Slichter
V	own model
X	direction
Y	direction
Z	direction
exp	measured
g	gas
o	apparent cross-sectional area or effective gas flow surface
ε	microchannel
0	ambient pressure

knowing those mechanisms, it is possible to evaluate process conditions that accompany hydrodynamics of gas flow through this type of materials, and, consequently, to thoroughly describe hydrodynamic conditions of gas flow through materials and porous deposits.

The assessment of gas permeability through porous deposits is significant for both process and technological reasons. In both cases, numerous attempts are made to search for effective methods for predicting permeability of porous materials, as well as effective ways of measuring and verifying the methods of this assessment. The methods used to measure gas permeability through porous deposits are very diversified in the literature, and it may be assumed that the only common feature of these methods is the structure of samplers, although there is no uniformly unified methods of this assessment. An additional difficulty in this regard is that the samples used in the research are of a different form and shape, and most often they are model deposits, which do not always correspond to the real conditions. A somewhat different aspect is that the assessment of gas permeability is generally carried out in one selected flow direction of the prepared sample, which in relation to porous natural materials leads to large quantitative errors. This state of affairs does not facilitate the transfer of measurement results to the real conditions, nor does it facilitate the establishment of clear criteria for the transfer of scale. This results in the individualisation of methods for assessing the gas permeability through porous deposits that are usually based on experimental formulas.

The examples included in the studies (Blicharski & Smulski, 2012; Darcy, 1856; Jansen, Meertens, & Wilms, 1964; Mertas, Sobolewski, & Różycki, 2013; Miura & Nishioka, 1992; Nomura et al., 2010; Popielski, 2000; RILEM Technical Recommendation, 1999; Roga & Wnękowska, 1952; Rozhkova, 2010; Shi, Xu, Shi, & Zhou, 2008; Tucker & Everitt, 1992, pp. 40–61; Śliwiński & Tracz, 2013) were used to characterise and analyse the selected methods for measuring the gas permeability through various porous materials with:

a) grain structure (soil, filter deposits),
b) frame structure (pumice, coal, coke and other coal chars),
c) capillary-porous structure (ceramic materials, concrete).

Virtually, in all the cases described in the literature there is no uniform view of the possibility of using in the gas flow hydrodynamics description the criteria for the assessment of gas permeability (gas flow stream). In addition, in the reference books there are considerable variations in the approach to the experimental assessment of the permeability parameters. It hinders to a great extent the possibility of the research results, which, consequently, leads to difficulties in adapting the existing computational models. An additional problem is the proper assessment of the nature of the flow and the actual flow parameters resulting from the structure of the porous deposit.

2. Materials and method

The permeability research was conducted upon a number of diversified types of materials, the average porosity of which ranged from 22% to 56%. Most of them were coal chars (cokes) from the thermal processing of hard coal and there are also materials like partially melted waste rocks (including volcanic ones), natural and synthetic pumice and porous agglomerate. The research material comprised various types of solid frame structures thoroughly analysed in the study by Wałowski and Filipczak (2016a,b).

For selected types of porous material, a physical assessment of the structure of the tested materials was made. This was done on the basis of the available scanning image (SEM), as exemplified by the ex situ carbonisation sample shown in Fig. 1. To evaluate such a complete picture field, selected areas were selected to allow the graphical identification of the structure of the porous surface. For this purpose, specialized software for object-oriented image analysis was used, Iris-MediCom Wroclaw. In the example shown in Fig. 1, three such identification fields A, B and C are considered as representative of the cross-section. In each selected field (generally 1000 × 1000 μm), the free space circuit in a given plane is graphically displayed, both in the form of microchannels and slots. Using the graphical software tools, the total pore size and average size of each plot were determined for each designated area A, B, C, and on this basis the average porosity of each field analysed and average pore diameter were determined. Then, for each sample analysed in this way, mean values of these samples were determined – corresponding to this analysis, the sample results are presented in Table 1.

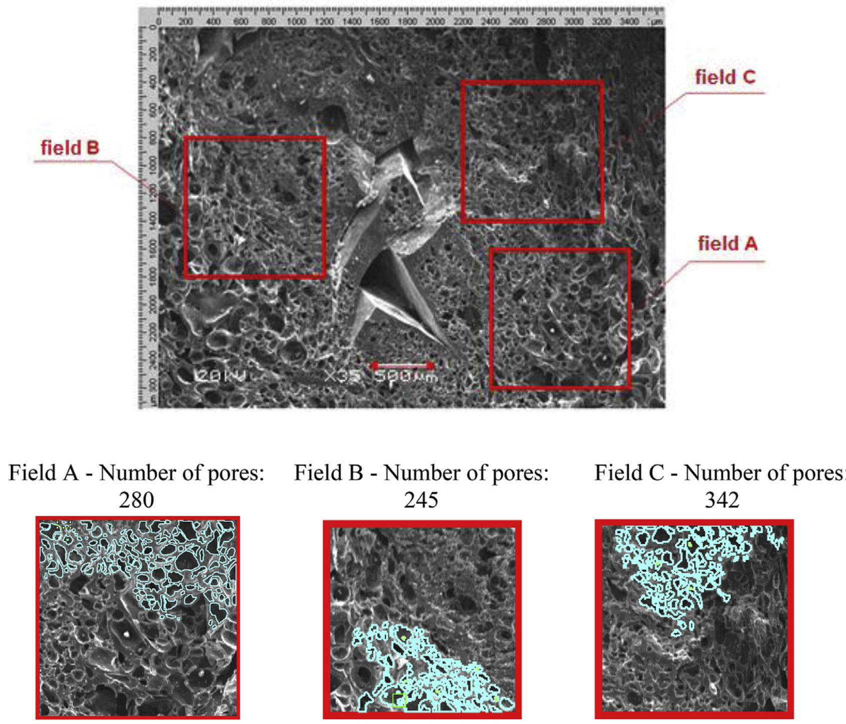

Fig. 1. Identification of the SEM image of the char *ex situ* (sample IV-1), with fields (A, B, C) marked for free space estimation (acc. Table 1, item 4a).

Table 1
Characteristics of research material.

Property characteristics			
Research material (a sample)		Parameters	
		Absolute porosity ε_b, %	Equivalent pore diameter d_e, μm
Char *ex situ* (IV)	4a	37.5	61.5
	4b	40.4	67.1
	4c	49.0	76.6
	average	42.3	68.4

2.1. Experimental stand

Experimental studies were carried out on a specially measuring set-up (Filipczak, Krause, & Wałowski, 2017), the general scheme of which is shown in Fig. 2a. An essential element of this bench is a flow module (Fig. 2b), in which a specimen of porous material (1) is placed. The specimens were cube shaped (Fig. 2c), and the module flow channel design allowed for the measurements of permeability for each of the three main flow directions (X, Y, Z) by rotating the cubic specimen in a selected plane of the measuring cell (Wałowski & Filipczak, 2016a,b).

To obtain the research objective, the detailed experimental tests were conducted to assess the gas permeability of porous materials with the diversified structure and the diversified process characteristics (Table 2). The gas permeability research was conducted by using air as a working medium.

2.2. Scope and research methodology

To assess the hydrodynamics of the gas flow through porous materials, tests were carried out with respect to cubic-shaped samples Fig. 2c. Tests were conducted with reference to gas (air) to the extent of the permeability stream resulting from the reference pressure.

An independent evaluation of the pressure drop permeability function on the porous bed was made, assuming the XYZ directed flow characteristic of the cubic sample. It is worth mentioning that for the cubic-shaped sample permeability measurements were conducted independently for each selected flow direction by rotating this sample in the selected plane X, Y, Z of the measurement cell.

The purpose of the study is to assess the permeability that resulting from the pressure inducing this flow. In each case, this characteristic is determined by calculating the impact of the available overpressure on the obtained gas stream or vice versa - the impact of the gas stream on the value of this overpressure that corresponds to a decline in this stream pressure. In the latter case, this corresponds to the determination of complete resistances of the gas flow through such deposit.

3. Results and discussion

Methods of measuring and evaluating the coefficient of gas permeability through porous deposits are very diversified as they most often result from the measurement methods adapted to specific process conditions. Additional limitations in this assessment are due to the large complexity of hydrodynamic phenomena that accompany the flow of gases through the porous media, which in turn entails difficulties in generalising this phenomenon.

As an example Figs. 3 and 4 compare values of the permeability coefficient according to various models with respect to various tested materials for the gas flow to the Z direction.

As you can see, in all cases very diversified results are obtained, both in terms of the calculation method used and the type of the material used. Just for coal char *in situ* (Fig. 3) three characteristic tendencies may be determined for changes in values of the permeability coefficient together with the pressure increase: decreasing, stable and increasing. According to Darcy's law (Balhoff & Wheeler, 2009; Darcy, 1856; Teng & Zhao, 2000) (1) the

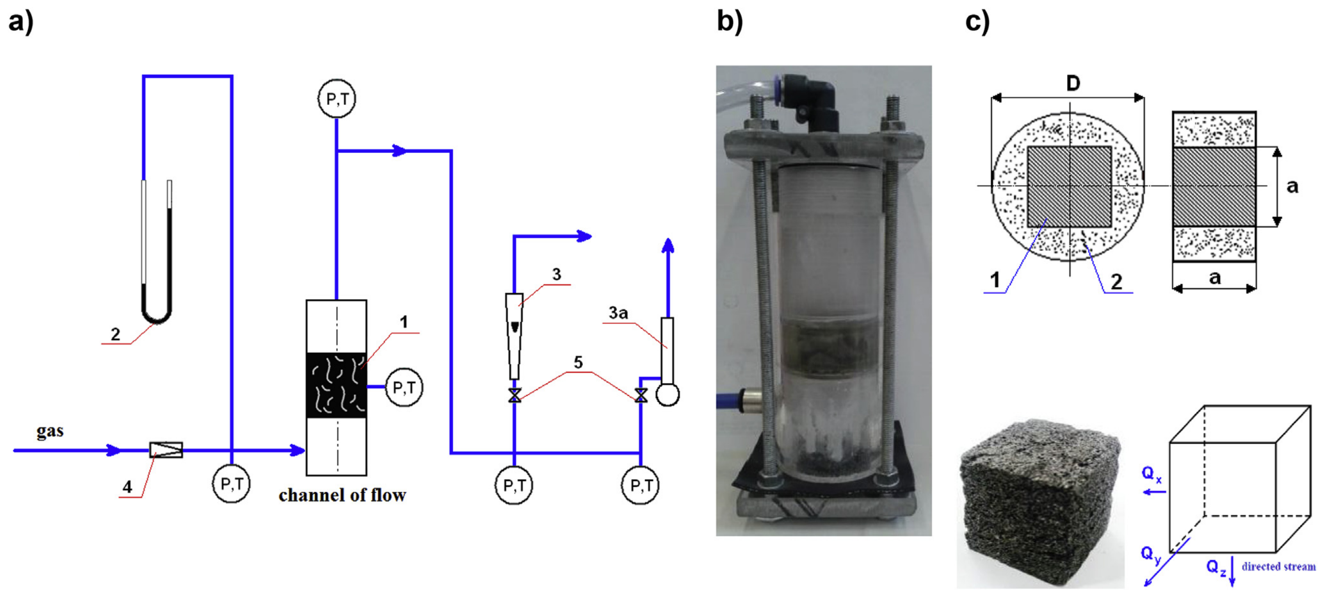

Fig. 2. Diagram of the test set-up with its equipment: a) measuring system: 1 - porous material (specimen), 2 - manometer, 3 - rotameter (3a - bubble flowmeter for the smaller flow rates), 4 - gas pressure regulator, 5 - control valve; b) flow module channel; c) measuring cell: 1 - sealing frame, 2 - specimen (D - inner diameter of flow module, a - specimen size).

decreasing tendency shows the greater effect of choking the gas stream compared with the allowable pressure value. Similar results are achieved by ASTM (Standard Test Method for Permeability of Rocks by Flowing Air, 2001) (2) but in this case permeability coefficient values are considerably lower.

$$K_D = \frac{u \cdot L \cdot \eta}{\Delta P} \tag{1}$$

where: K_D – permeability coefficient acc. Darcy, m^2; u - apparent velocity, m/s; L – flow path length describing the porous bad height, m; η - fluid viscosity, Pa·s; ΔP – pressure drop, Pa;

$$K_{ASTM} = \frac{2 \cdot Q \cdot p_0 \cdot \eta \cdot L}{\left(\Delta P^2 - p_0^2\right) \cdot \varepsilon \cdot F} \tag{2}$$

where: K_{ASTM} – permeability coefficient acc. ASTM, m^2; Q – volume flow rate, m^3/s; p_0 - ambient pressure, Pa; η - fluid viscosity, Pa·s; L – flow path length describing the porous bad height, m; ΔP – pressure drop, Pa; F – cross-sectional area, m^2; ε - porosity.

Other studies do not give such clear results and the constant values of this coefficient determined according to the method of Dullien (Dullien & Azzam, 1973; Dullien, 1992; Macdonald, El-Sayed, Mow, & Dullien, 1979) (3) and the method of Slichter (Deming & Anderson, 2005; Popielski, 2000; Slichter, 1899, 1905) (4) are explained by the fact that those methods only include structural parameters of the porous material. The similar notation is observed for the models of Forchheimer (Forchheimer, 1901; Hansen, 2007; Huang & Ayoub, 2008; Meyer, Bazan, & Walls, 2013; Peszyńska, Trykozko, & Sobieski, 2010; Scheidegger, 1974) (5) and of Brinkman (Brinkman, 1949; Hansen, 2007; Ranz & Marshall, 1952; Wałowski, Filipczak, & Krause, 2013) (6), where the slight growth tendency results from considering gas characteristics in those models;

$$K_{Du} = \frac{d_e^2 \cdot \varepsilon^3}{180(1-\varepsilon)^2} \tag{3}$$

where: K_{Du} – permeability coefficient acc. Dullien, m^2; d_ε – diameter of microchannel, m; ε – porosity;

$$K_S = 7,8 \cdot \varepsilon^{3,26} d_e^2 \tag{4}$$

where: K_S – permeability coefficient acc. Slichter, m^2; m; ε – porosity; d_ε – diameter of microchannel;

$$K_F = \frac{u \cdot \eta}{\frac{\Delta P}{L} - \left(\rho \cdot \beta \cdot u^2\right)} \tag{5}$$

where: K_F – permeability coefficient acc. Forchheimer, m^2; u – apparent velocity, m/s; η – fluid viscosity, Pa·s; ΔP – pressure drop, Pa; L – flow path length describing the porous bad height, m; ρ – density, kg/m^3; β – parameter in this case indicates the deviation from the linear Darcy relationship, as caused by the additional kinetics effects, 1/m^2.

$$K_B = \frac{u \cdot \eta}{\frac{\Delta P}{L} - \left(\rho \cdot \beta \cdot u^2\right) - u \cdot \eta} \tag{6}$$

where: K_B – permeability coefficient acc. Brinkman, m^2.

On the other hand, the completely different changes to the permeability coefficient may be observed for the model of Szczełkaczew (Pisarczyk, 2005; Szczełkaczew, 1948; Wałowski & Filipczak, 2016a,b):

$$K_{Sz} = \frac{u \cdot \eta}{g \cdot \rho} \tag{7}$$

where: u – apparent velocity, m/s; η – fluid viscosity, Pa·s; g – gravitational acceleration, m/s^2; ρ – density of gas, kg/m^3.

In this case, the description of hydrodynamics seems to be the closest to the physical structure of coal chars, i.e. their considerable fissuring. This indicates an increase in intensity of permeability along with an increase in pressure, without any choking effects.

It is also worth emphasizing the results referring to the model of Szczełkaczew (7) converted for materials of various diversity – Fig. 4. Very small values of the permeability coefficient for such materials as coke, pumice, coal char *ex situ* prove that the structure of those materials is closed for the gas flow (blind and closed pores)

Table 2
Test results in conditions: air, 18 °C.

Research material		Char *in situ*		Coke Zdzieszowice (Poland)		Coke Illawarra (Australia)	
Sample number		I-1		II-1		II-26	
No.	Reference pressure P_o, MPa	Gas stream $V \cdot 10^3$, m^3/s	Resistance flow ΔP_{exp}, kPa	Gas stream $V \cdot 10^3$, m^3/s	Resistance flow ΔP_{exp}, kPa	Gas stream $V \cdot 10^3$, m^3/s	Resistance flow ΔP_{exp}, kPa
direction of gas flow: X							
1	0.04	0.272	25.5	0.010	11.6	0.031	13.0
2	0.08	0.484	64.2	0.027	47.9	0.078	39.5
3	0.1	0.571	83.5	0.042	71.8	0.106	60.9
4	0.12	0.664	104.4	0.049	93.8	0.142	85.5
5	0.16	0.787	131.3	0.060	131.3	0.189	122.8
direction of gas flow: Y							
1	0.04	0.157	21.9	0.011	11.6	0.078	9.7
2	0.08	0.319	61.3	0.019	47.9	0.218	38.7
3	0.1	0.384	80.6	0.027	70.8	0.272	61.3
4	0.12	0.470	102.8	0.038	99.8	0.376	87.1
5	0.16	0.571	132.5	0.049	128.7	0.506	124.0
direction of gas flow: Z							
1	0.04	0.286	22.7	0.027	10.6	0.031	8.9
2	0.08	0.531	63.2	0.042	48.9	0.103	39.4
3	0.1	0.628	83.5	0.063	69.7	0.142	60.2
4	0.12	0.726	104.3	0.085	92.4	0.171	86.2
5	0.16	0.816	124.6	0.121	130.6	0.243	117.0
average values XYZ							
1	0.04	0.230	23.4	0.015	11.3	0.046	10.4
2	0.08	0.434	62.9	0.028	48.2	0.133	39.2
3	0.1	0.516	82.5	0.041	70.8	0.174	60.8
4	0.12	0.610	103.8	0.054	95.3	0.230	86.3
5	0.16	0.715	129.4	0.070	130.2	0.313	121.2
Research material		Char *ex situ*		Natural pumice		Synthetic pumice	
Sample number		VI-1		XIII-1		XIV-1	
No.	Reference pressure P_o, MPa	Gas stream $V \cdot 10^3$, m^3/s	Resistance flow ΔP_{exp}, kPa	Gas stream $V \cdot 10^3$, m^3/s	Resistance flow ΔP_{exp}, kPa	Gas stream $V \cdot 10^3$, m^3/s	Resistance flow ΔP_{exp}, kPa
direction of gas flow: X							
1	0.04	0.004	19.0	0.009	7.2	0,005	17.6
2	0.08	0.011	62.8	0.025	37.4	0,011	42.0
3	0.1	0.017	83.9	0.034	64.1	0,014	63.8
4	0.12	0.020	98.0	0.045	90.4	0,020	86.1
5	0.16	–	–	0.067	126.7	0,024	127.9
direction of gas flow: Y							
1	0.04	0.015	19.3	0.006	10.6	0,025	4.9
2	0.08	0.024	62.5	0.013	39.2	0,063	35.2
3	0.1	0.034	81.4	0.017	62.8	0,092	58.0
4	0.12	0.042	101.1	0.024	86.5	0,121	82.1
5	0.16	0.049	132.1	0.042	128.3	0,164	119.4
direction of gas flow: Z							
1	0.04	0.002	23.4	0.001	18.2	0,001	6.4
2	0.08	0.004	59.1	0.002	45.8	0,009	41.9
3	0.1	0.005	81.4	0.003	65.6	0,013	66.8
4	0.12	0.006	99.1	0.004	91.4	0,017	88.7
5	0.16	0.007	129.7	0.005	124.4	0,024	129.7
average values XYZ							
1	0.04	0.005	20.5	0.003	11.2	0.005	8.2
2	0.08	0.010	61.4	0.009	40.6	0.019	39.6
3	0.1	0.014	82.2	0.012	64.1	0.025	62.8
4	0.12	0.017	99.4	0.016	89.4	0.034	85.6
5	0.16	0.018	130.9	0.024	126.5	0.045	125.6

Research material		Porous sinter	
Sample number		XV-1	
No.	Reference pressure P_o, MPa	Gas stream $V \cdot 10^3$, m^3/s	Resistance flow ΔP_{exp}, kPa
direction of gas flow: X			
1	0.04	0.078	7.2
2	0.08	0.276	40.4
3	0.1	0.376	63.2
4	0.12	0.477	87.5
5	0.16	0.600	128.6

(*continued on next page*)

Table 2 (*continued*)

Research material		Porous sinter	
Sample number		XV-1	
No.	Reference pressure P_o, MPa	Gas stream $V \cdot 10^3$, m^3/s	Resistance flow ΔP_{exp}, kPa
direction of gas flow: Y			
1	0.04	0.060	4.7
2	0.08	0.225	29.7
3	0.1	0.380	66.8
4	0.12	0.474	90.7
5	0.16	0.600	127.7
direction of gas flow: Z			
1	0.04	0.078	7.3
2	0.08	0.247	39.1
3	0.1	0.358	61.8
4	0.12	0.452	85.3
5	0.16	0.600	128.7
average values XYZ			
1	0.04	0.071	6.3
2	0.08	0.248	36.1
3	0.1	0.371	63.9
4	0.12	0.467	87.8
5	0.16	0.600	128.3

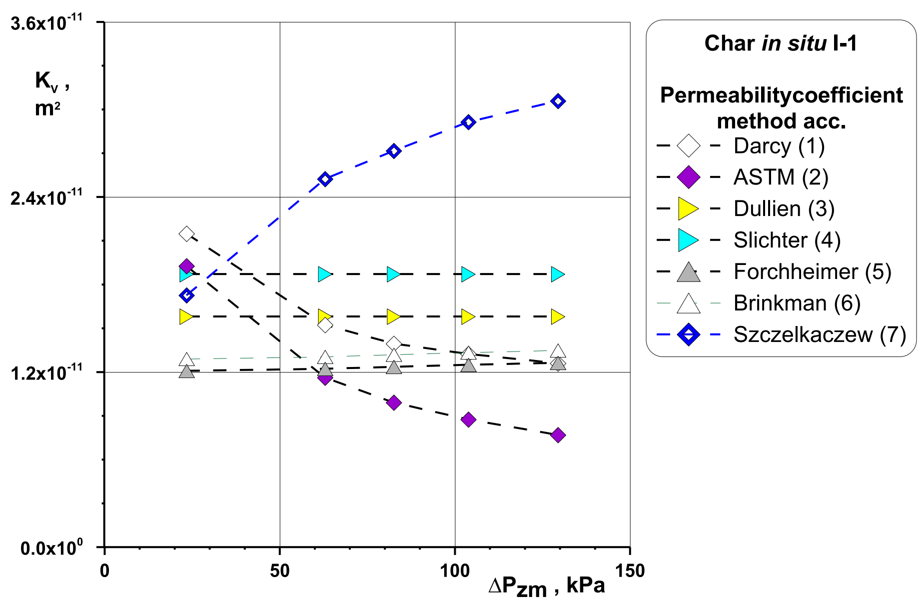

Fig. 3. Coefficient of permeability for Z direction of flow with respect to different calculation methods.

despite relatively high porosity (e.g. 63÷88% for pumice). On the other hand, such materials as coal char *in situ* and polyamide agglomerate - despite a relatively small porosity (32–42%) - are characterised by a highly intensive gas flow, which proves, on the one hand, their gap-porous structure (coal char) and, on the other hand, the full free surface for this flow and the regular structure of the material (porous polyamide).

In the context of large discrepancies, and numerous limitations in the use of models known in the literature, both in the aspect of porous structure and in the approach to gas hydrodynamics evaluation, such materials were attempted to develop their own model to assess the permeability coefficient.

As a rule, the own model was referred to the alternative approach to the assessment of the pressure drop as a result of local resistances as described by the equation:

$$\Delta P = \xi \frac{\rho \cdot u^2}{2} \tag{8}$$

where: ΔP – pressure drop, Pa; ξ – coefficient of drag flow; ρ – density, kg/m^3; u – velocity, m/s;

which, with respect to the coefficient of resistance and velocity to the conditions described by the porosity value (ε) may be as follows:

$$\Delta P = \xi_\varepsilon \frac{\rho_g \cdot u_\varepsilon^2}{2} \tag{9}$$

where: ΔP – pressure drop, Pa; ξ_ε – coefficient of drag flow; ρ_g – density of gas, kg/m^3, u_ε – apparent velocity for the value calculated for porosity, m/s.

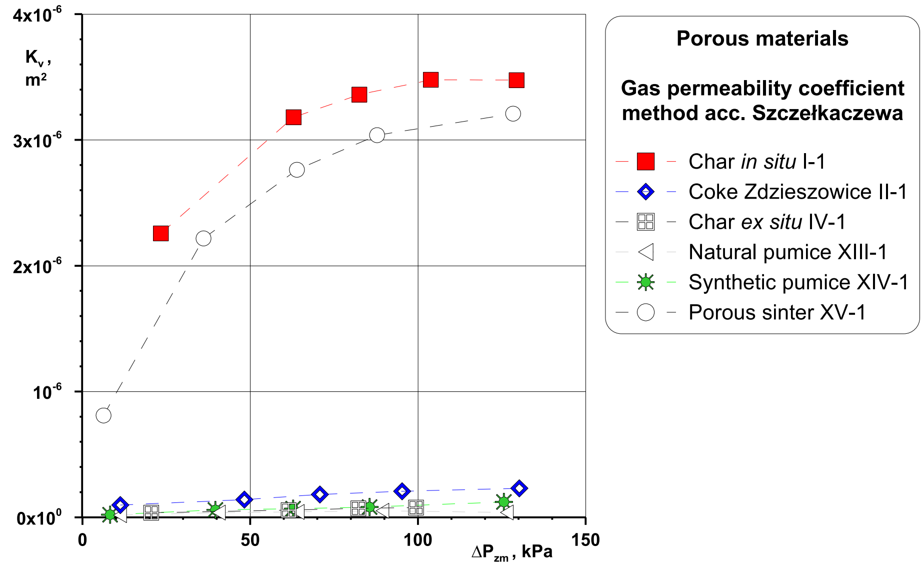

Fig. 4. Coefficient of gas permeability for Z direction of flow for porous materials according to the method of Szczelkaczew (7).

The transformation of this equation leads to

$$\Delta P = \xi_\varepsilon \frac{\rho_g \cdot u_\varepsilon^2}{2} = \frac{1}{2}\xi_\varepsilon \cdot \rho_g \left(\frac{Q_g}{A_o}\right)^2 \tag{10}$$

where: ΔP – pressure drop, Pa; ξ_ε – coefficient of drag flow; ρ_g – density of gas, kg/m^3, u_ε – apparent velocity for the value calculated for porosity, m/s; Q_g – gas stream, m^3/s; A_o – apparent cross-sectional area or effective gas flow surface, m^2;

$$\frac{\Delta P}{\frac{\xi_\varepsilon \rho_g}{2}} = \left(\frac{Q_g}{A_o}\right)^2 \tag{11}$$

$$\sqrt{\frac{2\Delta P}{\xi_\varepsilon \rho_g}} = \frac{Q_g}{A_o} \tag{12}$$

$$Q_g = A_o \sqrt{\frac{2\Delta P}{\xi_\varepsilon \rho_g}} \tag{13}$$

and further

$$Q_g = \sqrt{A_o^2 \frac{2\Delta P}{\xi_\varepsilon \rho_g}} = \sqrt{\frac{2A_o^2}{\xi_\varepsilon}}\sqrt{\frac{\Delta P}{\rho_g}} \tag{14}$$

where the effective surface of the gas flow results from the deposit porosity (ε) which, converted into the total cross-section of the flow channel, equals to

$$A_o = \varepsilon A \tag{15}$$

where: A_o – apparent cross-sectional area or effective gas flow surface, m^2; ε – porosity; A – total cross-section of the flow channel, m^2.

It is easy to notice that the expression

$$\sqrt{\frac{2A_o^2}{\xi_\varepsilon}} \tag{16}$$

has the dimension of the surface, which in the hydrodynamic approach, enables considering them as the equivalent of the permeability coefficient. Therefore (from the definition)

$$K_V = \sqrt{\frac{2A_o^2}{\xi_\varepsilon}} \tag{17}$$

where: K_V – permeability coefficient, m^2; A_o – apparent cross-sectional area or effective gas flow surface, m^2; ξ_ε – coefficient of drag flow.

The gas stream is then described by the relation

$$Q_g = K_V \sqrt{\frac{\Delta P}{\rho_g}} \tag{18}$$

While the hydrodynamic parameters (gas stream, deposit pressure drop, deposit porosity and gas type) are known, the value of the defined permeability coefficient can be determined experimentally. Then,

$$K_V = \frac{Q_g}{\sqrt{\frac{\Delta P_{exp}}{\rho_g}}} \tag{19}$$

where: K_V – permeability coefficient, m^2; Q_g – gas stream, m^3/s; ΔP_{exp} – measured pressure drop, Pa; ρ_g – density of gas, kg/m^3.

When referring to this defined coefficient of permeability to the multi-plane flow directions X, Y, Z, (Q_X, Q_Y, Q_Z), for each of these we obtain

$$K_X = \frac{Q_X}{\sqrt{\frac{\Delta P_{exp}}{\rho_g}}}, \tag{20a}$$

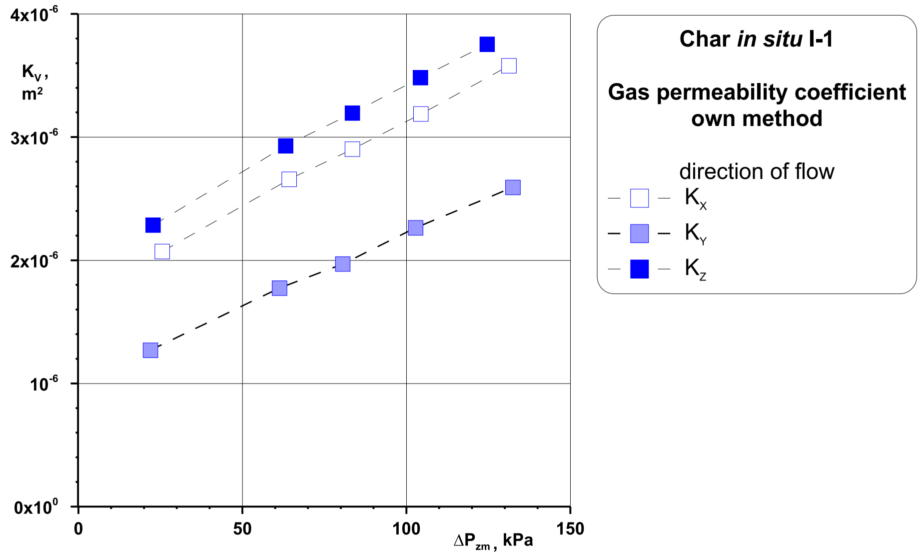

Fig. 5. Multidirectional gas permeability coefficients for char *in situ*, determined according to their own method (21).

$$K_Y = \frac{Q_Y}{\sqrt{\frac{\Delta P_{exp}}{\rho_g}}} \tag{20b}$$

$$K_Z = \frac{Q_Z}{\sqrt{\frac{\Delta P_{exp}}{\rho_g}}} \tag{20c}$$

The resulting average volume value of the permeability coefficient may be calculated as a square mean

$$K_V = \sqrt{\frac{{K_X}^2 + {K_Y}^2 + {K_Z}^2}{3}} \tag{21}$$

where: K_V – permeability coefficient, m^2; K_X – permeability coefficient for X-direction, m^2; K_Y – permeability coefficient for Y-direction, m^2; K_Z – permeability coefficient for Z-direction, m^2.

Contrary to some models, this formula does not consider the effect of gas viscosity on the permeability, but it is experimental in nature, thus capturing all the gas properties that result from both temperature and pressure changes.

Exemplary results resulting from the experimental determination of the permeability coefficient are shown in Fig. 5, in which a change in the value of this coefficient for a cubic coal char sample relative to the directed flow is shown. It is possible to observe the varying intensity of gas flow relative to each of the directions X, Y, Z, indicating the strong anisotropy of this type of material.

The characteristic feature of the relationship shown in Figs. 5 and 6 for describing this coefficient for other materials is the monotonous nature of the dependence of this coefficient with the increase in pressure. This indicates a proportional increase in permeability with increasing pressure, which is better suited to flow phenomena by porous structures. It also leads to the perception that this change is also conducive to the increase of the gas

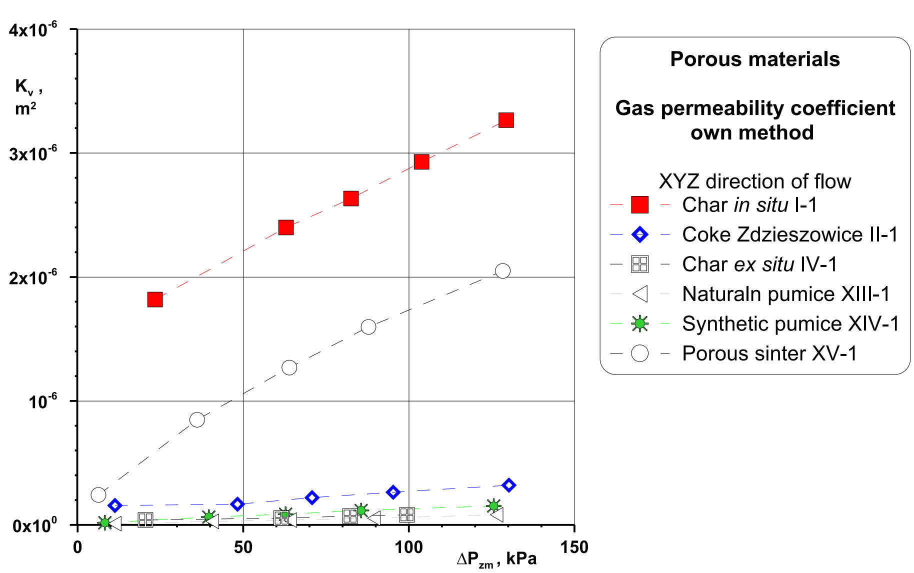

Fig. 6. Coefficient of gas permeability of porous materials determined according to one's own method (21).

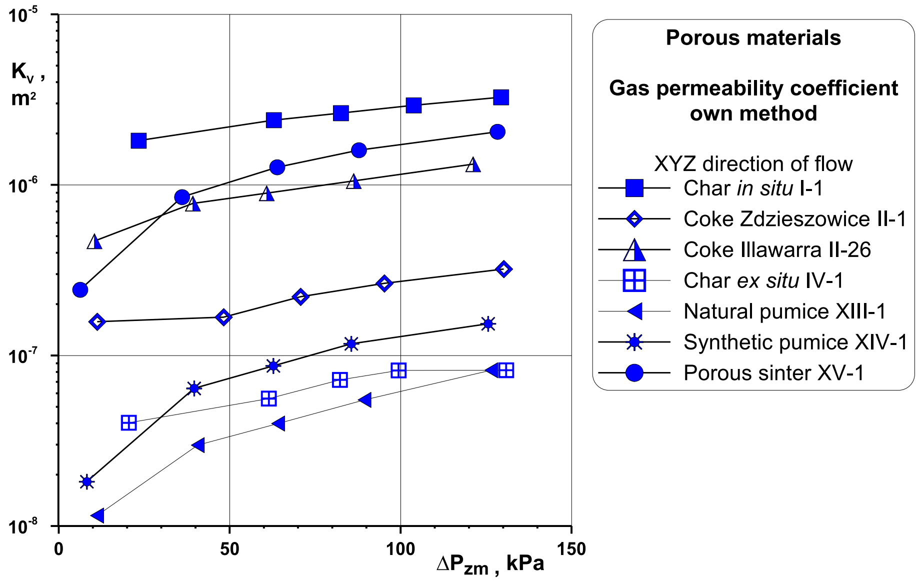

Fig. 7. Gas permeability coefficient of various materials determined according to own method (21) – half-logarithmic system.

stream. Of course, as is apparent from the direct measurement of this stream, many materials also exhibit a very low permeability level – Fig. 6 – which is derived from the structure of these materials. A slightly better look at this result is given in the semi-logarithmic set – Fig. 7.

In all the investigated cases it was found that the highest permeability was in coal char *in situ* (I-1), somewhat smaller porous polyamide (XV-1) and Illawarra coke (II-26), which may be regarded as medium permeable materials. Indirectly, this could be explained by the even scale of their porosity. The smallest permeability had pumice-group materials, coke and coal char *ex situ*.

With respect to the pressure drop in the porous deposit, the measurement results indicate that practically for each type of material the gas flow resistance grows with an increase in permeability. This suggests a fully free flow of gas, the stream of which results solely from the nature of the permeability of the deposit and is not related to the choking of the medium.

The similar results are received for the method of Szczełkaczew (7). On the basis of the comparison of the experimental points shown in Fig. 8 there is a high convergence of own results to this method, which may be derived from the assumptions of the method of Szczełkaczew (7), which refers to the analogy of laminar flow in small diameter tubes. This is also demonstrated by the similarity of the model with this method in the permeability assessment of materials with the lowest permeability coefficient such as pumice, coal char *ex situ* and coke (Fig. 9)

Physically, the permeability coefficient is a measure of the gas stream flowing through the porous material, and in formal terms it characterises the size of the cross-sectional area of the porous space open for such flow. The resulting values for this coefficient referenced to the mean gas velocity are shown in Fig. 9.

In the physical interpretation, the results of these studies are consistent with the expectations, as indicated by the increasing nature of the gas permeability changes with increasing flow rates.

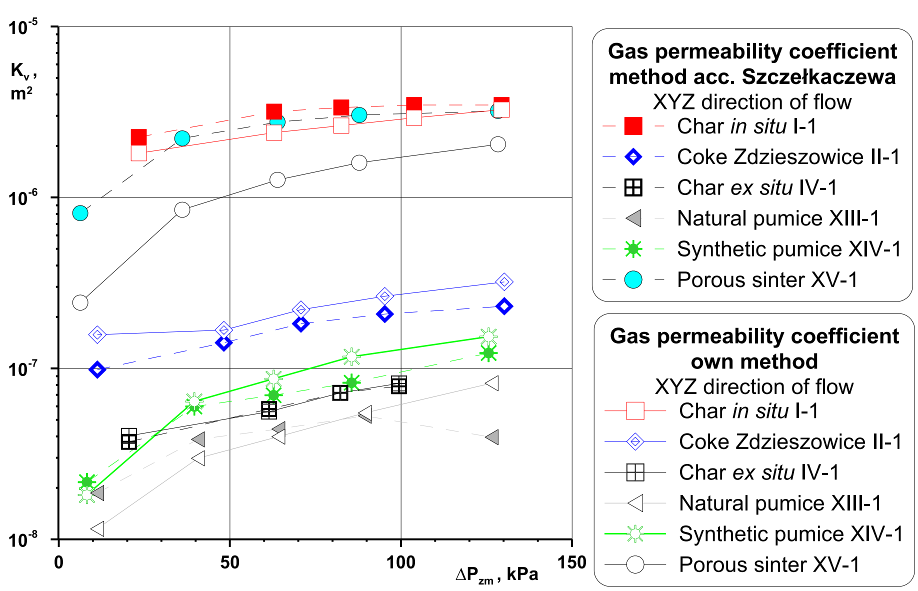

Fig. 8. Distribution of experimental points for gas permeability coefficient according to method of Szczełkaczew (7) and own method (21) – half-logarithmic system.

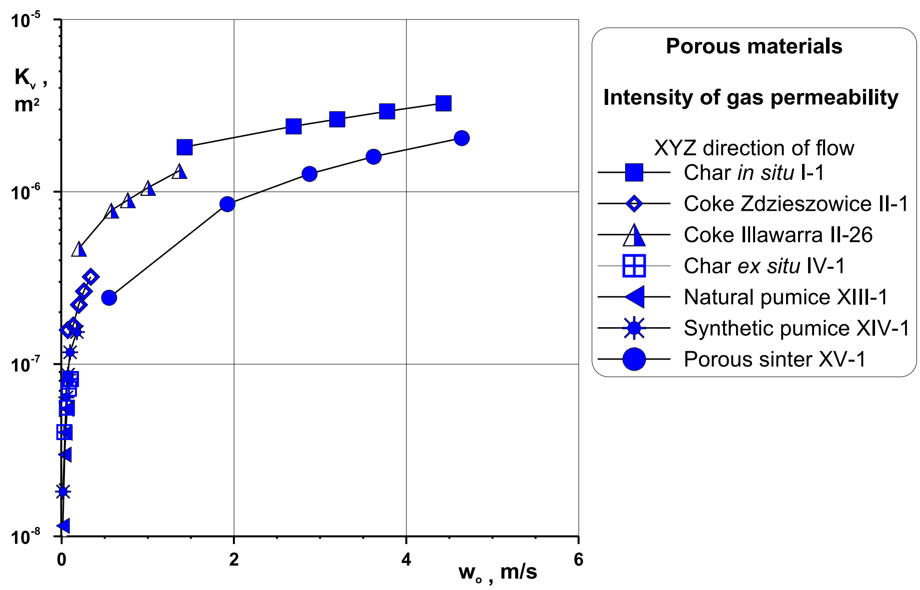

Fig. 9. Influence of gas velocity on the gas permeability of porous materials – half-logarithmic system.

4. Conclusions

The conducted experimental research results in the following conclusions:

The quantitative assessment of hydrodynamic parameters conducted with respect to books-based models, particularly in the aspect of flow resistances, has shown that none of the books-based models correctly correlate with the obtained research results. This is explained by great anisotropic properties of the tested materials and the restricted application of those models with respect to granular not frame-structured materials.

Our own calculative models developed on the basis of the acquired results basically describe a gas permeability co-efficient shows the consistence of the research results with the calculation results.

It has been proven that conditions of the quantitative assessment of hydrodynamics are affected by such characteristic parameters of the porous deposit as a porosity scale and anisotropic properties of its structure. Both of them considerably affect the gas permeability of the tested materials, which is considered in the theoretical assessment of this hydrodynamics.

Acknowledgements

The study conducted as part of the project financed by the National Centre for Research and Development conducted in the BIOSTRATEG program, contract No *BIOSTRATEG1/269056/5/NCBR/2015 dated 11 August 2015.*

References

Auriault, J. L., & Caillerie, D. (1989). Quelques remarques sur les methods d'homogénéisation. *Revue Française de Geotechnique, 49*, 43–50.

Auriault, J. L., & Royer, P. (1993). Ecoulement d'un gaz dans milieux poreux a double porosite: Mechanique des Sols et milieu poreux/Soil Mechanics and porous Media. *Comptes rendus de l'Académie des sciences. Série 2, Mécanique, Physique, Chimie, Sciences de l'univers, Sciences de la Terre, 317*(4), 431–436.

Auriault, J. L., Strzelecki, T., Bauer, J., & He, S. (1990). Porous deformable media saturated by a very compressible fluid: Quasi-statics. *European Journal of Mechanics, A/Solids, 9*(4), 373–392.

Balhoff, M., & Wheeler, M. F. (2009). A predictive pore-scale model for non-darcy flow in porous media. *SPE Journal, 14*(04), 579–587.

Barańska, J., & Sadowski, Z. (2015). Badania wpływu różnych dodatków na odzysk miedzi w procesie bioługowania rudy łupkowej w kolumnie [Study of the influence of various additives on the copper recovery at the column bioleaching of black shale ore]. *CUPRUM – Czasopismo Naukowo-techniczne Górnictwa Rud, 2*(75), 147–156.

Blicharski, J., & Smulski, R. (2012). Stanowisko laboratoryjne wypierania się płynów w ośrodkach porowatych w aspekcie sekwestracji CO_2 [Laboratory apparatus for fluids displacement in porous media in aspect of carbon dioxide sequestration]. *AGH Drilling, Oil, Gas, 29*(1), 89–96.

Brinkman, H. C. (1949). A calculation of the viscous force exerted by a flowing fluid on a dense swarm of particles. *Applied Scientific Research, 1*, 27–34.

Błaszczyk, M. (2014). *Badanie procesów migracji substancji ropopochodnych i ich emulsji w strukturach porowatych: Praca dokotorska* [Research upon processes of migration of petroleum substances and their emulsions in porous structures: doctoral thesis]. Łódź: Politechnika Łódzka, Wydział Chemiczny.

Darcy, H. (1856). *Les fontaines publiques de la ville de Dijon*. Paris: Victor Valmont.

Deming, D., & Anderson, M. P. (2005). The Wisconsin roots of ground water hydrology. *Ground Water, 43*(1), 142–145.

Dullien, F. (1992). *Porous Media: Fluid transport and pore structure* (2nd ed.). San Diego: Academic Press.

Dullien, F. A., & Azzam, M. I. (1973). Flow rate – pressure gradient measurement in periodically non-uniform capillary tubes. *AIChE Journal, 19*(2), 222–229.

Erust, C., Akcil, A., Gahan, S. C., Tusenuk, A., & Deveci, H. (2013). Biohydrometallurgy of secondary metal resources: A potential alternative approach for metal recovery. *Journal of Chemical Technology and Biotechnology, 88*(12), 2115–2132.

Filipczak, G., Krause, E., & Wałowski, G. (2017). *Układ do wyznaczania współczynnika przepuszczalności gazów przez porowate materiały o anizotropowej strukturze, zwłaszcza przez karbonizaty [System for determination the coefficient of gas permeability through porous materials with anisotropic structure, preferably through chars]*. About the grant of the patent was announced: 30.06.2017 WUP 06/17, Patent 225980. Warszawa: Urząd Patentowy Rzeczypospolitej Polskiej.

Forchheimer, P. (1901). Wasserbewegung durch Boden [Water movement through soil]. *Zeitschrift des Vereines Deutscher Ingenieuer, 5*(5), 1781–1788.

Gregg, D. W., & Edgar, T. F. (1978). Underground coal gasification. *American Institute of Chemical Engineers Journal, 24*(5), 753–781.

Hansen, T. E. (2007). *Flow in micro Porous silicon carbide*. Master Thesis. Lyngby: Technical University of Denmark: Department of Micro and Nanotechnology.

Huang, H., & Ayoub, J. (2008). Applicability of the Forchheimer equation for non-Darcy flow in porous media. *SPE Journal, 13*(01), 112–122.

Iliuta, I., & Larachi, F. (2005). Modeling simultaneous biological clogging and physical plugging in trickle-bed bioreactors for wastewater treatment. *Chemical Engineering Science, 60*(5), 1477–1489.

Janecki, D., Gąszczak, A., & Bartelmus, G. (2016). Modelling of the air purification from volatile organic compounds in a trickle-bed bioreactor. *Proceedings of ECOpole, 10*(2), 423–432.

Jansen, M. W. J., Meertens, J. L. J. G., & Wilms, A. H. (1964). Treibdruck der Kohle [Propellant pressure of the coal] I, II, III. *Brennst Chemie, 45*, 151–275.

Krause, E. (2009). *Metoda oceny zagrożenia metanowego projektowanych i eksploatowanych ścian w kopalniach węgla kamiennego [Methane hazard assessment method of designed and exploited walls in coal mines]*. Prace Naukowe Głównego Instytutu Górnictwa, 878. Katowice: Główny Instytut Górnictwa.

Macdonald, I. F., El-Sayed, M. S., Mow, K., & Dullien, F. A. L. (1979). Flow through porous media-the Ergun equation revisited. *Industrial Engineering Chemistry Fundamentals, 18*(3), 199–208.

Mertas, B., Sobolewski, A., & Różycki, G. (2013). Badania gazoprzepuszczalności warstwy plastycznej węgli jako czynnika wpływającego na wielkość generowanego ciśnienia rozprężania [Examination of the gas permeability of the carbonaceous layer as a factor influencing the size of the generated expansion pressure]. *Karbo, 2*, 163–171.

Meyer, B. R., Bazan, L. W., & Walls, D. (2013). Modeling of proppant permeability and inertial factor for fluid flow through packed columns. In A. P. Bunger, J. McLennan, & R. Jeffrey (Eds.), *Effective and sustainable hydraulic fracturing* (pp. 549–569). Rijeka, Croatia: InTech.

Miura, K., & Nishioka, K. (1992). Measurements of permeability of coal. Plastic and coke layers. *Cokemaking International, 4*(1), 45.

Nomura, S., Mahoney, M., Fukuda, K., Kato, K., Le Bas, A., & McGuire, S. (2010). The mechanism of coking pressure generation I: Effect of high volatile matter coking coal, semi-anthracite and coke breeze on coking pressure and plastic coal layer permeability. *Fuel, 89*(7), 1549–1556.

Peszyńska, M., Trykozko, A., & Sobieski, W. (2010). Forchheimer law in computational and experimental of flow through porous media at porescale and mesoscale. *GAKUTO International Series. Mathematical Sciences and Applications, 32*, 463–482.

Pisarczyk, S. (2005). *Mechanika gruntów [Mechanic of land]* (4th ed.). Warszawa: Oficyna Wydawnicza Politechniki Warszawskiej.

Popielski, P. (2000). *Model sufozji mechanicznej w ujęciu metody elementów skończonych: Praca doktorska [Model of sufficient mechanics in the finite element method: Doctoral thesis]*. Warszawa: Politechnika Warszawska.

Ranz, W. E., & Marshall, W. R. (1952). Evaporation from drops. Part I. *Chemical Engineering Progress, 48*(3), 141–146.

RILEM Technical Recommendation. (1999). Tests for gas permeability of concrete. TC 116-PCD: Permeability of concrete as criterion of its durability. *Materials and Structures, 32*(4), 174–179.

Roga, B., & Wnękowska, L. (1952). *Analiza paliw stałych*. Katowice: PWT.

Rozhkova, T. (2010). *Mid-term Report on realisation of RFCS project SPRITCO (no. RFCR-CT-2010-00006)*.

Scheidegger, A. E. (1974). *The physics of flow through porous media* (3rd ed.). Toronto: University of Toronto.

Shi, H., Xu, B., Shi, T., & Zhou, X. (2008). Determination of gas permeability of high performance concrete containing fly ash. *Materials and Structures, 41*(6), 1051–1056.

Slichter, C. S. (1899). *Theoretical investigations of the motion of ground waters*. U.S. Geological Survey 19th Annual Report, Part 2. Washington: Washington Government Printing Office.

Slichter, C. S. (1905). *Field measurements of the rate of movement of underground waters*. U.S. Geological Survey Water-Supply and Irrigation Paper No. 140, 122. Department of the Interior United States Geological Survey, Washington Government Printing Office.

Śliwiński, J., & Tracz, T. (2013). Wpływ szlifowania powierzchni betonu na ocenę jego przepuszczalności określanej metodą Torrenta [Impact of grinding of concrete surface on the evaluation of its permeability determined by the Torrent method]. In M. Kaszyńska (Ed.), *Awarie budowlane: Zapobieganie, diagnostyka, naprawy, rekonstrukcje: XXVI Konferencja Naukowo-Techniczna, Szczecin-Międzyzdroje, 21-24 maja 2013* (pp. 873–880). Szczecin: Wydawnictwo Uczelniane Zachodniopomorskiego Uniwersytetu Technologicznego.

Smoliński, A., Stańczyk, K., Kapusta, K., & Howaniec, N. (2013). Analysis of the organic contaminants in the condensate produced in the in situ underground coal gasification process. *Water Science & Technology, 67*(3), 644–650.

Stachowiak, A., Nowak, J., & Sztromwasser, E. (2011). Złoża węgla brunatnego w regionie Legnicy-Ścinawy i technologie ich zagospodarowania [The lignite deposits in the Legnica-Ścinawa area the methods of their exploitation]. In A. Żelaźniewicz, J. Wojewoda, & W. Cieżkowski (Eds.), *Mezozoik i kenozoik Dolnego Śląska* (pp. 121–135). Wrocław: WIND.

Standard Test Method for Permeability of Rocks by Flowing Air. (2001). *Designation: D 4525–4590, reapproved*. West Conshohocken: ASTM – American Society for Testing and Materials.

Strzelecki, T., Kostecki, S., & Żak, S. (2008). *Modelowanie przepływów przez ośrodki porowate [Flow modeling through porous media]*. Wrocław: Dolnośląskie Wydawnictwo Edukacyjne.

Szczełkaczew, W. N. (1948). *Elastic mode of water-bearing systems [In Russian]*. Moscow: M. Gostopekhizdat.

Teng, H., & Zhao, T. S. (2000). An extension of Darcy's law to non-Stokes flow in porous media. *Chemical Engineering Science, 55*(14), 2727–2735.

Tucker, J., & Everitt, G. (1992). Coking pressure – its causes, measurement and control. In *2nd International Cokemaking Congress Proceedings* (Vol. 2). London: The Institute of Materials.

Wałowski, G., & Filipczak, G. (2016a). Gazoprzepuszczalność materiałów porowatych o anizotropowej strukturze [Gas permeability of porous materials with an anisotropic structure]. *Inżynieria i Aparatura Chemiczna, 55*(6), 245–250.

Wałowski, G., & Filipczak, G. (2016b). Assessment of process conditions associated with hydrodynamics of gas flow through materials with anisotropic internal structure. *Journal of Sustainable Mining, 15*, 156–169. http://dx.doi.org/10.1016/j.jsm.2017.03.003.

Wałowski, G., Filipczak, G., & Krause, E. (2013). Hydrodynamika przepływu gazu w porowatych strukturach karbonizatu w aspekcie technologii podziemnego zgazowania węgla. [Hydrodynamics of gas flow in porous carbonisate structures in the aspect of underground coal gasification technology]. In *Młodzi dla Techniki 2013. Wybrane problemy naukowo-badawcze chemii i technologii chemicznej* (pp. 253–270). Płock: Politechnika Warszawska.

Łydżba, D. (1991). Constitutive equation of gas-coal medium. *Studia Geotechnica et Mechanica, 13*(3–4), 51–62.

Łydżba, D. (2002). Zastosowania metody asymptotycznej homogenizacji w mechanice gruntów i skał [Applications of asymptotic homogenization in soil and rock mechanics]. *Prace Naukowe Instytutu Geotechniki i Hydrotechniki Politechniki Wrocławskiej. Monografie, 74*(23), 274, 274.